

CCA-765

539.172.3:620.193  
Conference Paper

## The Application of Mössbauer Spectroscopy to the Study of Corrosion\*

H. Leidheiser, Jr., G. W. Simmons, and E. Kellerman

Center for Surface and Coatings Research, Lehigh University, Bethlehem, Pennsylvania, U.S.A.

Received January 15, 1973

The Mössbauer spectroscopic methods that have been used for studying corrosion phenomena include transmission, emission and reflection (scattering) techniques. Each of these techniques provides unique capabilities for studying a wide range of applied and fundamental corrosion problems. The various Mössbauer spectroscopic techniques are described and compared, and applications of each method to corrosion studies are reviewed.

### INTRODUCTION

The purpose of this paper is to describe and to compare various Mössbauer spectroscopic techniques useful in corrosion studies. A review of the applications to problems in corrosion is also given. Although Mössbauer spectroscopy is applicable to a limited number of metals, the technique nevertheless has provided and will continue to provide a tool for practical and fundamental corrosion studies primarily of iron, tin, cobalt, and alloys containing these elements. The theoretical basis of the Mössbauer effect and the specific chemical and physical information derivable from  $\gamma$ -ray resonance spectroscopy have been reviewed elsewhere<sup>1,2</sup>. The basic principles required for an understanding of the various experimental approaches will, however, be considered in the present review.

Te considerable information available in the literature on the characterization by Mössbauer spectroscopy of iron and tin compounds provides a strong basis for applying  $\gamma$ -ray resonance spectroscopy to corrosion studies. The isomer shift, quadrupole splitting, and magnetic hyperfine splitting have been measured for a large number of organic and inorganic compounds of iron and tin including many of the compounds formed during corrosion of these metals. In particular, the oxides and hydroxides of iron have been studied extensively. Some of the chemical and physical properties of oxides that are important to corrosion phenomena, such as the relationship between the stoichiometry of  $\text{Fe}_3\text{O}_4$  and its conductivity<sup>3</sup> have been determined by Mössbauer spectroscopy<sup>4</sup>. In many cases direct quantitative measurement can be made of corrosion products that consist either of a single oxide phase or of a complex mixture of corrosion species. A particular advantage of the Mössbauer technique is that spectra can be obtained from either amorphous or crystalline corrosion products, provided that the Mössbauer nuclei are rigidly bound. The deviations of the hyperfine interactions from the bulk values can provide useful information about

\* Lecture prepared for the *III International Conference on the Chemistry at Interfaces*, Rovinj, Yugoslavia, June 27—30, 1972.

corrosion products. In particular, the particle size of magnetic materials can be readily determined, since the magnetic hyperfine interaction tends to collapse with decreasing particle volume. In small particles,  $< 100 \text{ \AA}$ , the magnetic moment fluctuates between the easy directions of magnetization in a time comparable to the lifetime of the excited state of the Mössbauer nucleus. The net result of this fluctuation is to average the hyperfine field to zero, and consequently, in the case of  $\text{Fe}^{57}$ , the normal six-line spectrum collapses to a single line, or to a double line when quadrupole effects are present.

In addition to the conventional transmission spectroscopy, both reflection (scattering) and emission spectroscopy have been applied to corrosion studies. The latter two approaches provide a high surface sensitivity and a means for non-destructive studies of thin corrosion films. The excited Mössbauer nucleus, following resonance absorption, releases energy by a number of radiative and/or non-radiative transitions. Table I lists for  $\text{Fe}^{57}$  these transitions, cor-

TABLE I

*Radiative and Radiationless Transitions Associated with De-excitation of  $\text{Fe}^{57}$  [16]*

Radiation	Energy (kev)	Transition Probability
Resonant gamma ray	14.4	0.09
M-shell conversion electron	14.3	0.01
L-shell conversion electron	13.6	0.09
K-shell conversion electron	7.3	0.81
$K_{\alpha}$ X-ray	6.3	0.24
KLL Auger electron	5.4	0.57

responding transition probabilities, and the energy associated with each transition. Reflection spectroscopy employs experimental methods that detect the emission of the resonantly produced radiation or electrons in the absorber. Emission spectroscopy is performed by incorporating the source isotope, for example  $\text{Co}^{57}$ , into the specimen under study, and obtaining the spectrum of the emitter by transmission with a single line absorber. The experimental arrangements used in each of the spectroscopic techniques are summarized in Fig. 1.

Each of the methods mentioned above is described further in the following sections along with a review of representative corrosion studies that have employed each technique.

### *Transmission Spectroscopy*

Transmission Mössbauer spectroscopy is directly applicable to corrosion studies of thin metal foils and the major application has been in studies of relatively thick corrosion products  $10^4$  to  $10^6 \text{ \AA}$  in thickness. Corrosion of bulk material can be studied by preparing a suitable specimen for transmission from corrosion layers that have been removed from the substrate. The relative

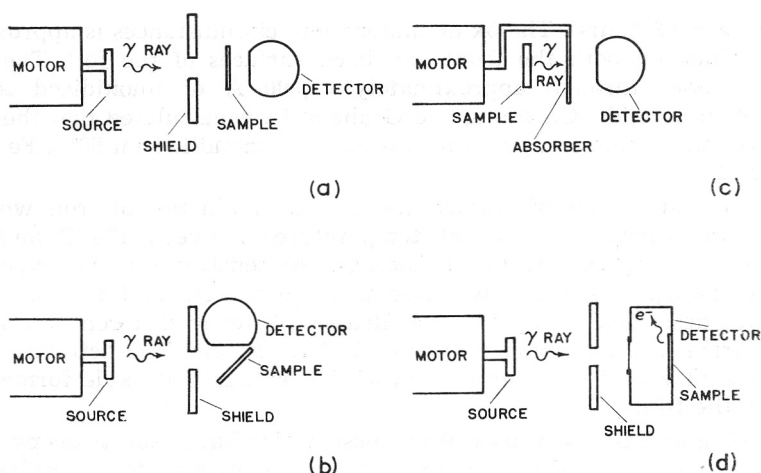


Fig. 1. Experimental arrangements used in Mössbauer experiments (a) transmission, (b) X-ray and  $\gamma$ -ray scattering, (c) emission and (d) X-ray and electron scattering.

concentrations for any number of phases, 1, 2, 3...n can be determined from the following relationship:

$$\frac{N_1}{N_2} = \frac{A_1}{A_2} \frac{f_1}{f_2}$$

where for each phase,  $N$  is the number of atoms/cm<sup>3</sup> of the Mössbauer element,  $A$  is the area under the resonance peak and  $f$  is the recoil-free fraction. The absolute concentration of a given phase in a specimen can be determined from the area under the resonance peaks. Absolute quantitative analysis is, however, more difficult since it is necessary to determine accurately the background counts and fundamental parameters such as the recoil-free fraction, linewidth of the source, and the resonance cross section.

A typical example of the information obtained from transmission spectroscopy is represented in Fig. 2, which shows an absorption spectrum of a  $0.95 \times 10^{-3}$  cm. thick iron foil oxidized in pure oxygen at 1 atmosphere pressure

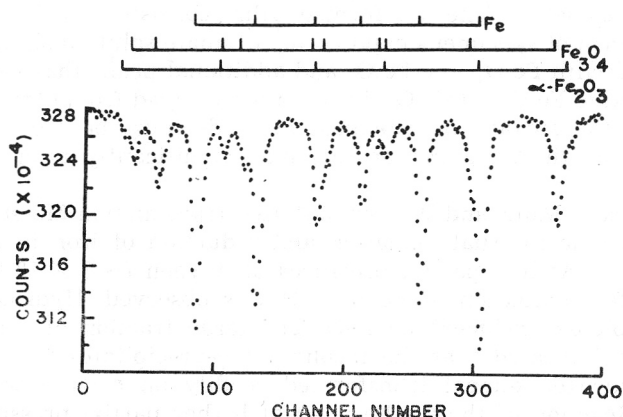


Fig. 2. Transmission spectrum of oxidized iron foil (Adapted from Channing and Graham<sup>5</sup>).

and 500 °C for 3.2 hours<sup>5</sup>. The oxide under these circumstances is approximately 30,000 Å. thick on both the front and back surfaces of the foil. The gamma ray thus passes through approximately 63,000 Å of unoxidized iron and 60,000 Å. of iron oxide. Channing and Graham<sup>5</sup> have calculated that the relative areas under the absorption peaks in this case are metallic iron 66%, Fe<sub>3</sub>O<sub>4</sub> 32%, and Fe<sub>2</sub>O<sub>3</sub> 2%.

Pritchard and Dobson<sup>6</sup> studied the corrosion kinetics of iron which was heated in deoxygenated water at temperatures between 180 °C and 290 °C. The surface was enriched in Fe<sup>57</sup> to increase the sensitivity of the experiments. Magnetite, Fe<sub>3</sub>O<sub>4</sub>, was the only oxide phase observed, and the rate of film growth was described by  $dy/dt = ky^3$ . Reaction rates at different temperatures gave an Arrhenius activation energy of 15.6 kcal/mole. The activation energy was associated with the decomposition of the ferrous hydroxide formed at the surface of the film.

Channing and Graham<sup>5</sup> used transmission Mössbauer spectroscopy to study oxidation of Fe<sub>3</sub>O<sub>4</sub> to  $\alpha$ -Fe<sub>2</sub>O<sub>3</sub> in oxygen and to investigate the reduction by iron of  $\alpha$ -Fe<sub>2</sub>O<sub>3</sub> to Fe<sub>3</sub>O<sub>4</sub> during annealing of partially oxidized foils in vacuum. An activation energy of 49 kcal/mole was determined for the conversion of Fe<sub>3</sub>O<sub>4</sub> to  $\alpha$ -Fe<sub>2</sub>O<sub>3</sub>, and an activation energy of 31 kcal/mole was measured for iron transport through Fe<sub>3</sub>O<sub>4</sub>. The relatively low activation energies were attributed to short-circuit diffusion processes.

The formation of rust on iron in the presence of saturated water vapor at room temperature and by periodic immersion in calcium chloride solution was studied by Dezsi, Vertes, and Kiss<sup>7</sup>. The rust formed in water vapor consisted of 50% by wt.  $\alpha$ -Fe<sub>2</sub>O<sub>3</sub>, ~ 40%  $\gamma$ -FeOOH, and ~ 10%  $\beta$ -FeOOH, and corrosion in the salt solution produced equal amounts of  $\beta$ -FeOOH and  $\gamma$ -FeOOH. The conclusions derived from spectroscopy were supported by thermoanalytical measurements.

Bancroft, Mayne, and Ridgway<sup>8</sup> removed the air-formed oxide and the oxide formed upon immersion of iron in chromate solution by stripping the films from the iron substrate in a CH<sub>3</sub>OH-Br medium. The stripped films were collected on filter paper and the ferrous bromide was removed by heating the samples at 300 °C in dry nitrogen. The product was broken up, sandwiched between two pieces of adhesive tape, and the Mössbauer pattern determined in transmission geometry. The air-formed film consisted of Fe<sub>3</sub>O<sub>4</sub> —  $\gamma$ -Fe<sub>2</sub>O<sub>3</sub>. Mössbauer spectra of specimens exposed to chromate solution showed resonance lines associated with Fe<sub>3</sub>O<sub>4</sub> —  $\gamma$ -Fe<sub>2</sub>O<sub>3</sub> and additional peaks that were attributed to the mixed oxide Fe<sub>2</sub>O<sub>3</sub> · 3 Cr<sub>2</sub>O<sub>3</sub>. Information derived from corrosion products stripped from the surface by chemical methods must be viewed with some reservation, since the stripping process may significantly alter the corrosion products.

Gonser, Grant, Muir, and Wiedersich<sup>9</sup> used transmission Mössbauer spectroscopy to follow the internal oxidation and reduction of iron in a copper-iron (2.2 at. %) alloy. At low partial pressures of oxygen (~ 3 × 10<sup>-4</sup> torr) and at 850 °C incomplete oxidation of Fe to FeO was observed. Hydrogen annealing at 900 °C completely reduced the FeO. The large fraction of  $\alpha$ -iron observed after reduction indicated that the incoherent  $\gamma$ -precipitates that were formed during the hydrogen anneal transformed readily on cooling without plastic deformation. Reaction of the Cu-Fe alloy at higher partial pressure of oxygen (0.2 torr) produced complete oxidation to Fe<sub>3</sub>O<sub>4</sub>. From the intensities of the

$\text{Fe}^{+3}$  and  $\text{Fe}^{+2}$  resonance lines, the stoichiometry of the magnetite corresponded to  $\text{Fe}_{2.87}\text{O}_4$ . Attempts to oxidize the specimens further to  $\gamma\text{-Fe}_2\text{O}_3$  resulted in the formation of  $\text{CuFeO}_2$  (delafossite).

In recent studies by Pritchard, Haddon, and Walton<sup>10</sup> the Mössbauer spectra of corrosion products removed from a mild steel, high temperature water circuit in a nuclear reactor were compared with the spectra obtained from hydrothermal decomposition of  $\text{Fe}(\text{OH})_2$ . The similarity of the spectra suggested that the decomposition of  $\text{Fe}(\text{OH})_2$  to  $\text{Fe}_3\text{O}_4$  is an important reaction in determining the nature of the products formed during start-up, and that the relatively large  $\text{Fe}_3\text{O}_4$  particles are in part responsible for the subsequent protection of the mild steel from further corrosion.

### *Reflection Spectroscopy*

Any of the resonantly produced radiation or electrons listed in Table I may be used for reflection (or scattering) spectroscopy. The choice of radiation used in reflection spectroscopy for corrosion studies depends upon the specific application. The detection of emitted 14.4 keV or 6.3 keV X-rays is suitable for studying advanced stages of corrosion, and K-conversion electron detection is more applicable to investigating the formation of thin corrosion films. The major advantage of reflection spectroscopy is that bulk specimens can be studied while the corrosion products are still attached to the substrate. Another significant advantage of the scattering techniques is the relatively high signal-to-noise ratio. In transmission experiments the background count rate (or nonresonance count rate) is largely due to the  $\gamma$ -rays that have not been absorbed by the specimen, consequently, the total background counts do not differ appreciably from the number of incident  $\gamma$ -rays. In scattering geometry the detector is shielded from the direct radiation from the source, and the background, therefore, is principally from the non-resonantly produced radiation from Rayleigh, Compton and photoelectron scattering in the absorber. In addition, the cross sections for the non-resonant phenomena in scattering experiments are generally a few orders of magnitude lower than the resonant effects, and consequently higher signal-to-noise is possible than for transmission. Details of the experimental methods, relative surface sensitivities, and the quantitative capabilities of each of the scattering techniques are described in the following sections along with a review of the applications of each method to corrosion studies.

*Resonant Scattering of  $\gamma$ -Rays.* — Resonantly scattered  $\gamma$ -rays have not been considered seriously for use in corrosion studies because the high probability for internal conversion reduces the efficiency for detecting the Mössbauer effect. Since internal conversion produces a higher yield of resonant radiation than possible for re-emission of  $\gamma$ -rays, most reflection Mössbauer spectroscopy has employed the scattered radiation associated with internal conversion.

The experimental arrangement used in  $\gamma$ -ray scattering experiments is shown in Fig. 1b. Pulse height selection is used to minimize the background produced in the specimens by Compton and photoelectron scattering of the 122 keV and 132 keV  $\gamma$ -rays from the source. Rayleigh-scattered 14.4 keV  $\gamma$ -rays, however, are not distinguishable in energy from the Mössbauer-scattered  $\gamma$ -rays, and the theoretical limit of signal-to-noise is determined by the ratio of Mössbauer to Rayleigh scattering.

Meisel<sup>11</sup> has used the  $\gamma$ -ray scattering technique to determine that the corrosion product on iron exposed to 100% relative humidity was  $\beta$ -FeOOH, and Collins<sup>12</sup> compared the  $\gamma$ -ray and X-ray scattering techniques for determining the composition of rust on iron and steel.

*Resonant Scattering of Conversion X-Rays.* — The de-excitation of the Mössbauer nuclei, following resonance absorption, takes place either by re-emission of  $\gamma$ -rays or by the emission of s-electrons (internal conversion). In the case of Fe<sup>57</sup>, the  $\gamma$ -ray yield is 0.09 and the K-conversion yield is 0.81. The de-excitation of the ionized atom produce  $K_{\alpha}$ —X-rays, 6.3 keV, with a fluorescence yield of 0.24. The yield for resonantly produced X-rays is, therefore, approximately a factor 2 higher than for the re-emission of resonant  $\gamma$ -rays. Background generated by Rayleigh scattering of incident photons that have the same energy as the resonantly produced radiation is a problem for both  $\gamma$ -ray and X-ray scattering experiments. In the case of X-ray reflection spectroscopy, however, the Rayleigh scattering of incident X-rays can be minimized by mounting a non-resonant energy dependent filter between the source and specimen. In other words, the intensity of conversion X-rays from the source can be reduced with an appropriate filter without significantly reducing the 14.4 keV  $\gamma$ -radiation. Background from Compton scattering of the incident  $\gamma$ -radiation can be minimized by pulse height selection. The principle source of background in X-ray scattering is, therefore, from X-ray fluorescence produced in the scatterer by  $\gamma$ -radiation. The K-conversion X-rays have the same energy as the  $K_{\alpha}$  fluorescent X-rays, consequently, the theoretical limit of the signal-to-noise is the ratio of the cross sections for resonance absorption and for the production of non-resonant  $K_{\alpha}$ —X-rays.

Both of the experimental arrangements shown in Fig. 1b and 1d have been used in X-ray scattering experiments. The  $2\pi$  backscatter geometry shown in Fig. 1d is the most efficient detection method, since the scattered X-rays are detected over a large solid angle. Careful attention must be given to the design of the  $2\pi$ -detector, because all of the incident  $\gamma$ -radiation enters the counter. Swanson and Spijkerman<sup>13</sup> have determined the factors required for optimizing the count rate for scattered X-rays and for minimizing the background count rate produced by the incident radiation. Specimens were mounted inside the proportional counter and argon with 10% methane was used for a flow gas. The arrangement of the anode in the detector with respect to the incident  $\gamma$ -rays and to the specimen position was determined for optimum signal-to-noise operation.

The conventional scattering arrangement shown in Fig. 1b has the advantages that any portion of a large specimen can be readily studied and that the detector can be easily shielded from the incident radiation.

Quantitative analysis in scattering experiments requires a detailed description of both the attenuation of resonant  $\gamma$ -rays as they enter the absorber and the attenuation of resonantly produced X-rays that are emitted from specific depths within the scatterer. Hershkowitz and Walker<sup>14</sup> have derived theoretical expressions for the intensity of the resonant signal as a function of absorber thickness for forward scattering geometries. Terrell and Spijkerman<sup>15</sup> have made a similar formulation for back-scattering geometries. Fig. 3 shows the analysis of Terrell and Spijkerman for the intensity of back-scattered resonantly produced X-rays as a function of absorber thickness. Although

Fig. 3 shows intensity *vs.* thickness for a metallic iron absorber, functions can be derived for other absorbers (phases) by using the appropriate resonant absorption and mass absorption coefficients for the 14.4 keV and 6.3 keV photons, respectively. Thickness determinations for a single phase can be obtained by measuring the resonance line intensities from the specimens and determining thickness from the intensity *vs.* thickness curve after an initial calibration has been made of a known thickness. Accurate thickness determinations would be more difficult for multiphase systems, since the attenuation of scattered X-rays must be considered separately for each phase.

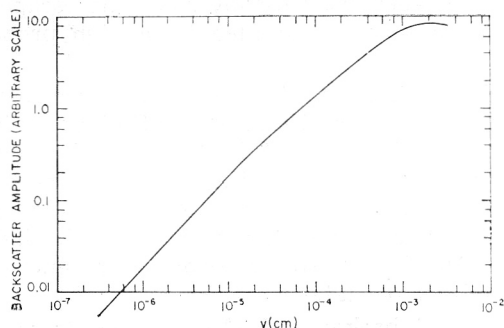


Fig. 3. Integrated conversion X-ray signal as a function of resonator thickness for backscattering. (Adapted from J. H. Terrell and J. J. Spijkerman<sup>13</sup>).

Swanson and Spijkerman<sup>13</sup> have experimentally determined the specimen depth that contributes to the Mössbauer spectrum of iron. A stainless steel absorber was covered with iron foils of known thicknesses, and the Mössbauer spectrum was obtained for each thickness. The calculated areas under the iron and stainless steel peaks showed that 78% of the backscattered X-ray signal came from the first  $5 \times 10^{-4}$  cm of sample depth and that 93% of the signal originated in the first  $1.3 \times 10^{-3}$  cm of absorber depth. The experimental values agree with the theoretical analysis shown in Fig. 3.

Although the resonant scattering of X-rays is a convenient method for applying Mössbauer spectroscopy to studies of corrosion, the technique has not been extensively employed. Two studies have been reported essentially to demonstrate the feasibility of the technique for characterizing corrosion products. Terrell and Spijkerman<sup>15</sup> used the X-ray detection method to study the corrosion product formed when a steel plate was exposed to HCl vapor. An excellent spectrum, interpreted as  $\beta$ -FeOOH, was observed. The film thickness was estimated to be  $2 \times 10^{-3}$  cm. Collins<sup>12</sup> used the technique to identify the corrosion products on a rusty window sash weight.

*Resonant Scattering of Electrons.* — The Mössbauer techniques described in the previous sections are primarily useful for studying the advanced stages of corrosion. On the other hand there are many corrosion conditions such as during low-temperature oxidation or anodic treatment that result in the formation of thin (10–500 Å) films. Resonant scattering of electrons offers the opportunity of obtaining from Mössbauer spectroscopy qualitative and quantitative information about the chemical and physical properties of thin corrosion layers.

For Fe<sup>57</sup> a probability of 0.81 is found for the emission of K-conversion electrons following resonance absorption of the 14.4 keV  $\gamma$ -ray. The K-conversion

electron energy of 7.3 keV is determined by the energy released in the nuclear transition less the binding energy of the K-electron. K-conversion produces an ionized atom which consequently releases energy by the emission of either photons or Auger electrons. The KLL Auger yield arising from K-level ionization is 0.57, and the Auger electron energy is 5.4 keV. If both conversion and Auger electrons are counted, the efficiency for detecting the Mössbauer effect by electron scattering is a factor of 15 higher than for  $\gamma$ -ray scattering and a factor of 7 higher than for X-ray scattering. The high yield of resonantly produced electrons of moderately low energy provides a means of studying surface layers by Mössbauer spectroscopy since the escape depth of electrons originating within an absorber is limited by a high probability for electron scattering.

The design and specifications for Mössbauer spectroscopy using electron detection have been described by Swanson and Spijkerman<sup>13</sup>. The experimental arrangement is shown in Figure 1d. A helium-10% methane flow gas provides a high electron-detection efficiency and a low efficiency for counting photons. It is essential that the specimen be mounted in the detector, since the high attenuation of electrons does not permit the use of windows. A method of conversion-electron Mössbauer spectroscopy with energy analysis of the emitted electrons is discussed later.

The main source of background electron counts is from photoelectron emission induced by  $\gamma$ -ray and X-ray interactions with the specimen and with the walls of the detector. Pulse height selection is used to eliminate electrons with energies outside the range of the 5.4 keV and 7.3 keV resonantly produced electrons. Photoelectron scattering of the 14.4 keV gamma rays produces photoelectrons and associated Auger electrons that have the same energies as the resonantly produced electrons, and consequently the theoretical limit of the signal-to-noise in electron scattering experiments is the ratio of the cross-section for resonance absorption with internal conversion to the photoelectron scattering cross-section of 14.4 keV  $\gamma$ -rays.

A complete theoretical description of electron back-scattering must include the attenuation of the incident resonant  $\gamma$ -rays and the attenuation of conversion and Auger electrons that are emitted from specific depths in the scatterer. Krakowski and Miller<sup>16</sup> have derived expressions for the area under resonance peaks and for electron intensity at maximum resonance for back-scattered K-conversion electrons. The integrals describing the electron signal are expressed in terms of the reduced resonator thickness  $\mu_K t$  and the ratio  $\mu_R/\mu_K$ , where  $\mu_K$  and  $\mu_R$  are the linear absorption coefficients for conversion electrons and for resonant  $\gamma$ -rays, respectively. Fig. 4 shows the dependence of the electron intensity on the reduced resonator thickness for two values of  $\mu_R/\mu_K$  corresponding to natural Fe<sup>57</sup> abundance (2%) and to complete Fe<sup>57</sup> enrichment. Note that the enriched resonator produces an electron signal approximately  $10^2$  greater than natural iron.

Values of the attenuation coefficient for electrons in different materials must be known to apply the analysis of Krakowski and Miller<sup>16</sup> to quantitative measurements. For electrons in the energy range of 5–15 keV Cosslett and Thomas<sup>17</sup> have shown experimentally that the mass absorption coefficient is nearly independent of  $Z$  and is proportional to  $E_0^{-3/2}$ :

$$(\mu/\rho)_K = 1.4 \times 10^{10} E_0^{-3/2}$$

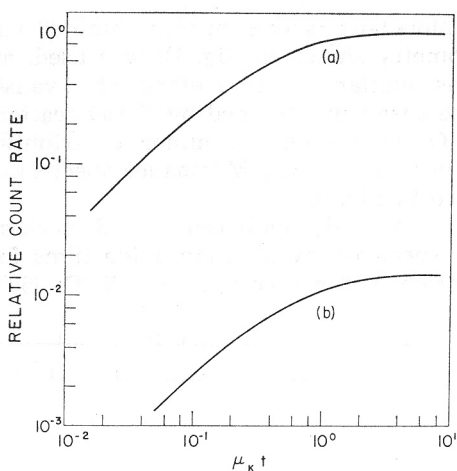


Fig. 4. Conversion-electron signal at maximum resonance as a function of reduced resonator thickness (a) completely  $\text{Fe}^{57}$ -enriched iron, (b) natural iron. (Adapted from Krakowski and Miller<sup>16</sup>).

where  $E_0$  is the initial electron energy. Calculated values of the K-conversion electron absorption coefficients,  $\mu_K$ , for iron and  $\text{Fe}_3\text{O}_4$  are  $1.75 \times 10^5 \text{ cm}^{-1}$  and  $1.16 \times 10^5 \text{ cm}^{-1}$ , respectively.

Calculated values for  $\mu_K$  and the functions in Fig. 4 can be used to estimate the percentage of the total electron signal that originates over a region at a specific depth from the surface. For an enriched iron absorber 65% of the total measured conversion electrons originate in the first 250 Å of the scatterer and for natural iron 65% of the signal comes from a surface region of 450 Å in depth. Swanson and Spijkerman<sup>13</sup> have experimentally determined the escape depth of conversion electrons in natural iron by taking Mössbauer spectra of known thickness of iron films that were deposited onto a stainless steel substrate. From the areas under the resonance peaks for iron and stainless steel, they calculated that 65% of the signal originated within the first 600 Å, a value that is somewhat higher than predicted by the analysis of Krakowski and Miller<sup>16</sup>. Although further theoretical and experimental work are required to resolve this discrepancy, the analysis presented in Fig. 4 is nonetheless useful for describing the conversion-electron intensity as a function of resonator thickness. Quantitative analysis of single phase systems is possible from the curves shown in Fig. 4 after the K-conversion electron intensity has been measured for a known thickness. Quantitative analysis for multiphase systems is complicated owing to differences in the attenuation of electrons in each phase.

A theoretical treatment applicable to experimental systems that count both conversion and Auger electrons must also include the electron signal arising from the KLL Auger transition. Since the Auger electrons have a lower initial energy, this electron signal originates within a region closer to the surface as compared to the depth over which conversion electrons are emitted. Krakowski and Miller<sup>16</sup> did not include the Auger electron contribution in their analysis.

The relative surface sensitivities of the X-ray and electron scattering methods can be demonstrated from experiments conducted in our laboratory. A  $\text{Fe}^{57}$ -enriched iron specimen was oxidized in dry synthetic air at 450 °C for

10 minutes and the Mössbauer spectrum was obtained with each method. The X-ray scattering geometry shown in Fig. 1b was used, and our electron scattering technique was similar to the method of Swanson and Spijkerman<sup>13</sup> described earlier. The spectrum obtained by X-ray scattering is given in Fig. 5 and shows that  $\text{Fe}_3\text{O}_4$  makes only a minor contribution. The  $\text{Fe}_3\text{O}_4$  oxide phase, however, is very clear in the Mössbauer spectrum obtained by electron scattering as indicated in Fig. 6.

Simmons, Kellerman, and Leidheiser<sup>18</sup> used back-scattered, conversion-electron, Mössbauer spectroscopy to study oxide films formed by the thermal oxidation of  $\text{Fe}^{57}$ -enriched iron specimens at 225 °C, 350 °C, and 450 °C. Möss-

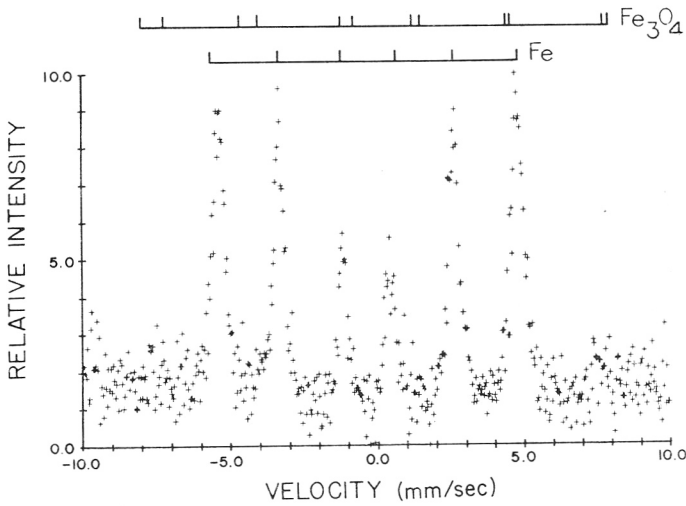


Fig. 5. Conversion X-ray Mössbauer spectrum of  $\text{Fe}^{57}$ -enriched iron oxidized at 450 °C for 10 minutes.

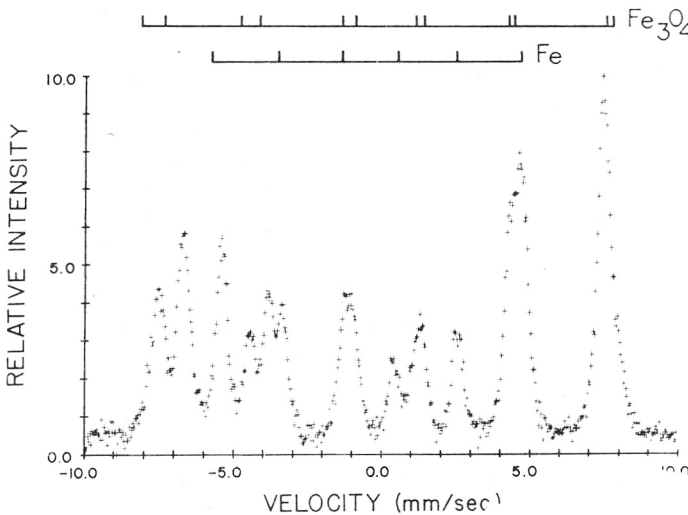


Fig. 6. Conversion-electron Mössbauer spectrum of  $\text{Fe}^{57}$ -enriched iron oxidized at 450 °C for 10 min

bauer spectra were obtained for oxide thicknesses ranging from approximately 50 to several hundred Angstroms. Fig. 7 shows the spectrum of iron after oxidation at 225 °C. The  $\text{Fe}_3\text{O}_4$  phase was estimated to be approximately 120 Å thick. The equal intensities of the A site and B site resonance lines indicate that the oxide formed at 225 °C is either non-stoichiometric  $\text{Fe}_3\text{O}_4$  corresponding to  $\text{Fe}_{2.91}\text{O}_4$  or a mixture of stoichiometric  $\text{Fe}_3\text{O}_4$  and  $\gamma\text{-Fe}_2\text{O}_3$ . In either case, it can be concluded that oxidation at 225 °C produces a cation-deficient  $\text{Fe}_{3-x}\text{O}_4$  oxide phase. Oxide growth at 225 °C was studied as a function of oxidation

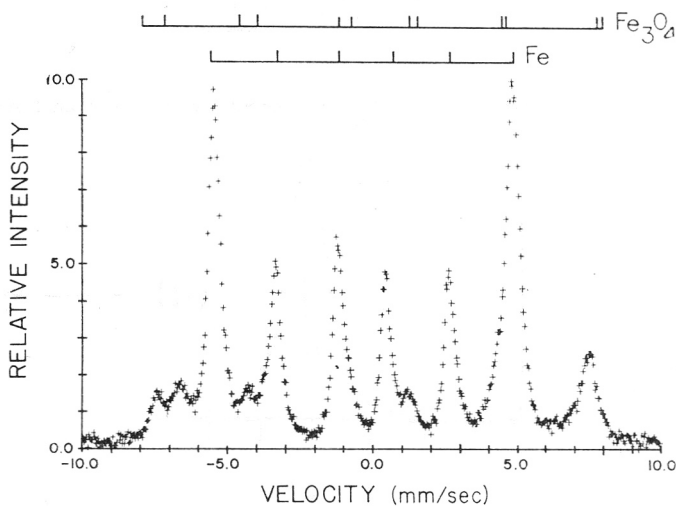


Fig. 7. Conversion-electron spectrum of  $\text{Fe}^{57}$ -enriched iron after oxidation at 225 °C. Oxide thickness is estimated to be approximately 120 Å.

time, and the increase in film thickness showed a logarithmic time dependence. Oxidation at 350 °C for short times produced a duplex film consisting of  $\text{Fe}_3\text{O}_4$  and  $\alpha\text{-Fe}_2\text{O}_3$ . Oxidation at 450 °C yielded a single oxide, nearly stoichiometric  $\text{Fe}_3\text{O}_4$ . The absence of  $\alpha\text{-Fe}_2\text{O}_3$  in short-time oxidation at 450 °C was attributed to an increased cation flux at the higher temperature.

Preliminary results have been reported by Onodera, Yamamoto, Watanabe, and Ebiko<sup>19</sup> on conversion electron Mössbauer studies of the corrosion of  $\text{Fe}^{57}$ -enriched iron in a solution of  $\text{NaNO}_2$  at pH 8. The principle corrosion product was identified as  $\alpha\text{-FeOOH}$ , but no estimate of the oxide thickness was given.

Bonchev, Jordanov, and Minkova<sup>20</sup> have shown that Mössbauer spectra of corrosion films as a function of depth can be obtained by energy analysis of K-conversion electrons since the electron energy losses are a function of escape depth. The Mössbauer effect in  $\text{Sn}^{119}$  was studied. The total probability for internal conversion in  $\text{Sn}^{119}$  is 0.95 and the L-conversion electron has an energy of 19.6 keV. The LMM Auger transition produces electrons with an energy of approximately 3.1 keV, consequently there is sufficient energy separation between resonantly produced electrons to provide spatial resolution over a significant depth from the surface. An electron spectrometer was used to focus conversion electrons of a definite energy onto a scintillation detector. The

experimental arrangement is shown schematically in Fig. 8. A  $\text{Sn}^{119}$ -enriched tin specimen was exposed to bromine vapor for approximately 10 seconds and the Mössbauer spectra of this sample were measured as a function of the magnetic focusing field of the spectrometer. Fig. 9 shows the spectra obtained

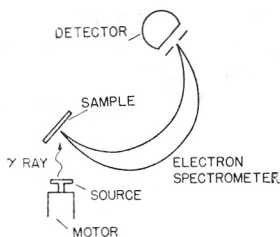


Fig. 8. Arrangement for Mössbauer scattering experiments with energy analysis of conversion electrons.

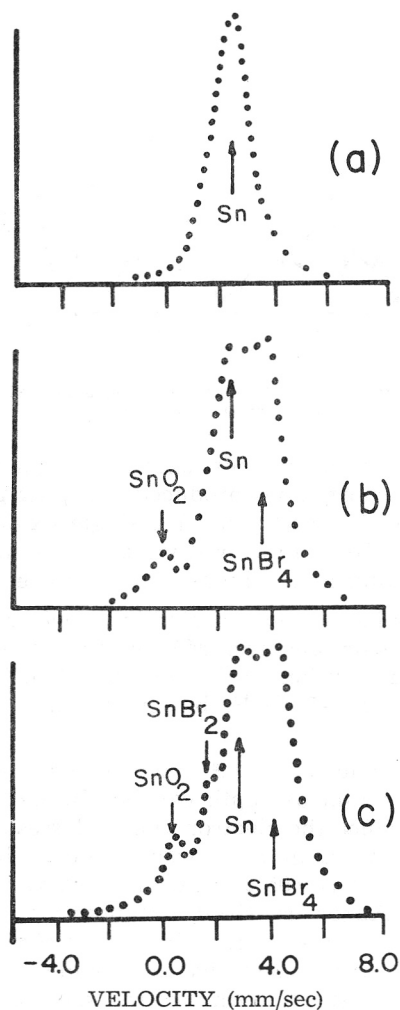


Fig. 9. Conversion electron spectra of Sn treated with bromine vapors. The energy of the electrons detected increases from (a) to (b). (Adapted from Bonchev, Jordanov, and Minikova<sup>20</sup>).

for electrons originating at different depths. For electrons with lowest energy a spectrum of  $\beta$ -Sn was produced, and for electrons of higher energies corrosion layers of  $\text{SnBr}_2$  and  $\text{SnBr}_4$  were detected. A similar experiment was performed with tin which was exposed to fuming nitric acid vapors. The relative intensities of the  $\beta$ -Sn and  $\text{SnO}_2$  Mössbauer resonance lines were measured as a function of electron energy. The relatively small dependence of the  $\beta$ -Sn/ $\text{SnO}_2$  intensity ratio on electron energy was attributed to a highly inhomogeneous oxide film.

Mössbauer spectroscopy of iron as a function of depth would also be possible by energy analysis of the K-conversion electrons, but no experimental work has yet been reported. Krakowski and Miller<sup>16</sup> have examined the scattering phenomena that determine the spatial resolution in electron-scattering Mössbauer experiments. They concluded that for measured electron energies  $E_K$  below approximately one half the initial conversion electron energy,  $1/2 E_{K_0}$ , the possibility of relating  $E_K$  to a specific depth into the resonator becomes poor. For conversion electron energies above  $1/2 E_{K_0}$ , however, the spatial-energy resolution is sufficient to permit Mössbauer spectra to be obtained from selected regions near a specimen surface. For  $\text{Fe}^{57}$ , the spatial resolution would be expected to degrade severely for  $E_K$  below 5.4 keV owing to the electron signal from the KLL Auger transition.

With the availability of high resolution electron spectrometers, it should be possible to obtain Mössbauer spectra with a depth sensitivity on the order of a few mean free path lengths of the K-conversion electrons.

### Emission Spectroscopy

The experimental arrangement used in emission spectroscopy is shown in Fig. 10. Emission spectra of the Mössbauer nuclei are obtained by doping

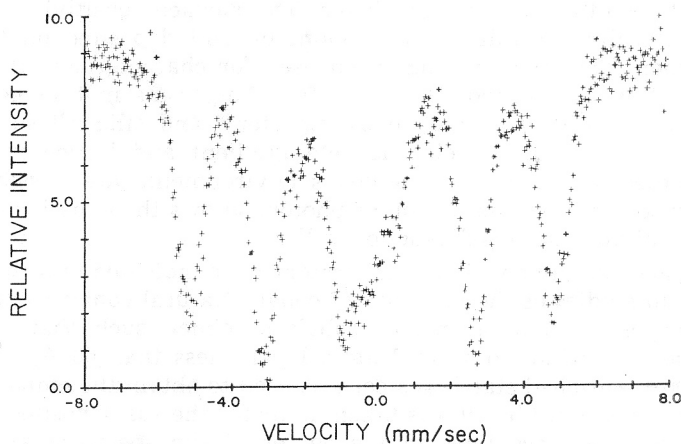


Fig. 10. Emission spectrum of »as deposited«  $\text{Co}^{57}$ -doped cobalt film approximately 50 Å thick.

the specimen with the source isotope, and performing a conventional transmission experiment with a single line resonant absorber. The discussion of emission spectroscopy will be limited in this review to studies with  $\text{Co}^{57}$ . The  $\text{Co}^{57}$  isotope decays to  $\text{Fe}^{57}$  by electron capture with a high probability of forming nuclear excited states that subsequently decay by emission of resonant  $\gamma$ -rays. The emis-

sion spectrum of a specimen, therefore, is from the  $\text{Fe}^{57}$  »impurity« atoms in the matrix under study, and the isomer shift, quadrupole splitting, and magnetic hyperfine splitting provide chemical and physical information about the host material. The signal-to-noise considerations and the quantitative capabilities are the same as for transmission spectroscopy described in an earlier section.

The application of the emission method for Mössbauer studies has the disadvantage that  $\text{Fe}^{57}$  may form non-equilibrium charge states as a result of the electron capture decay of  $\text{Co}^{57}$ . Electron capture produces an ionized K-level in  $\text{Fe}^{57}$ , and the Auger cascade which follows produces charge states up to + 7 in the valence levels<sup>21</sup>. If the non-equilibrium charges have a lifetime on the order of that for the nuclear excited states of  $\text{Fe}^{57}$  ( $\sim 10^{-7}$  s), then the emission spectrum will show resonance lines that are not produced by the intrinsic properties of the specimen. The stability of charges produced by Auger aftereffects depends upon the chemical and physical environment of the  $\text{Fe}^{57}$  nucleus. Normal  $\text{Fe}^{57}$  charge states are found when metals and alloys are doped with  $\text{Co}^{57}$ , since the highly mobile conduction electrons can rapidly return  $\text{Fe}^{57}$  to equilibrium. For insulating materials the charge equilibrium is slower and nonequilibrium charges as high as + 3 have been observed<sup>22,23</sup>. Stability of the charge states in insulators has been attributed to the influence of localized lattice defects such as the nonstoichiometry of the matrix. Although the possible presence of atypical charge states imposes a complication in the interpretation of spectra, emission spectroscopy can nevertheless be useful for obtaining important information of chemical and physical interest. Greenwood and Gibb<sup>23</sup> and Wertheim<sup>24</sup> have reviewed the work on emission spectroscopy of  $\text{Co}^{57}$ -doped metals and compounds.

For corrosion studies, the technique has the important advantage that investigations can be readily carried out *in situ* and with a possible surface sensitivity of less than one atomic layer. The surface sensitivity is obtained simply by carefully controlling the amount of  $\text{Co}^{57}$  deposited on the surface of the specimen. The technique has been used for characterizing the magnetic properties of thin evaporated films of a few Angstroms in thickness<sup>25</sup>. Mössbauer spectra of  $\text{Co}^{57}$  evaporated onto tungsten<sup>26</sup> and silicon<sup>27</sup> surfaces have provided information on the electric-field gradient and lattice vibrations at surfaces. Studies of corrosion in aqueous environments are possible *in situ*, since the low scattering cross section of photons allows the emission of resonant  $\gamma$ -rays from suitably designed reaction cells.

Preliminary experiments in our laboratory have indicated that the technique is applicable to studies of the passivity of cobalt. Natural cobalt containing  $\text{Co}^{57}$  was electrodeposited onto a smooth cobalt specimen such that the amount deposited was equivalent to several atom layers (less than 50 Å). A reference absorber of  $\text{Fe}^{57}$ -enriched stainless steel was used to obtain the emission spectra. The spectrum shown in Fig. 10 was taken in air for the »as deposited« specimen, and the strong resonance lines in the center of the spectrum are from the air-formed oxide. Assuming that the  $\text{Co}^{57}$ -doped cobalt film was relatively uniform in thickness, the oxide must have been less than 50 Å thick since some of the metal remained in the elemental state. The sample was cathodically polarized in 0.1 N sodium hydroxide, and the emission spectrum was taken while the sample was immersed in the electrolyte. Fig. 11 shows that cathodic treatment reduced the air-formed oxide, since the spectrum is essentially that of metallic cobalt. Anodic treatment of the same specimen while immersed in

the hydroxide solution yielded the pattern shown in Fig. 12. Practically all the surface cobalt was converted to the + 2 oxidation state as indicated by the isomer shift of the strong central peak. Studies are in progress to determine the extent of surface oxidation and the oxidation states of the surface atoms of cobalt as a function of polarization conditions in various electrolytes. Detailed analysis of the emission spectra may also yield chemical and physical information that is important to understanding passivation mechanisms.

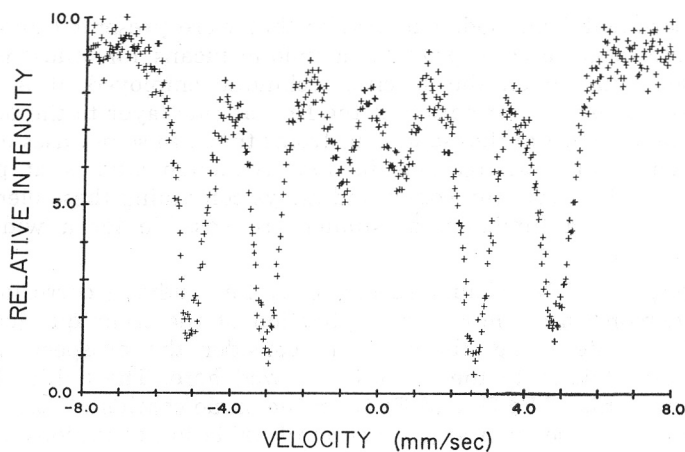


Fig. 11. Emission spectrum of specimen described in Fig. 10 during cathodic polarization in 0.1 M NaOH.

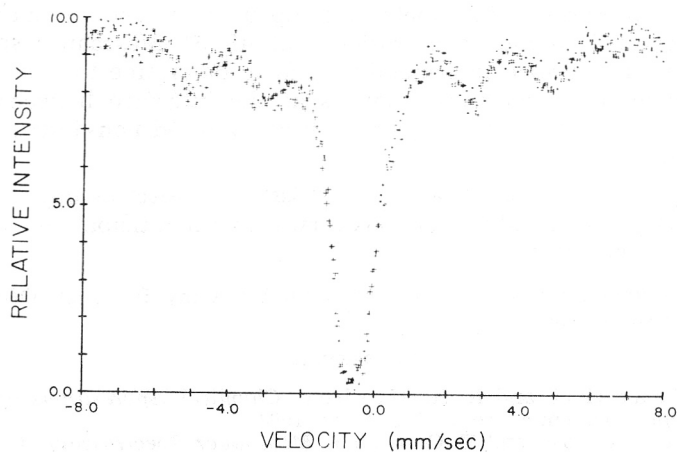


Fig. 12. Emission spectrum of specimen described in Fig. 11 during anodic polarization in 0.1 M NaOH.

Stress corrosion mechanisms, in part, involve the entry of hydrogen into the metal or alloy lattice. Mössbauer spectroscopy is applicable to metal-hydrogen systems and may provide information on the causes for changes in mechanical properties owing to the presence of hydrogen. Wertheim and Buchanan<sup>28</sup> have used the emission method to study the effects of hydrogen

charging on the Mössbauer spectrum of  $\text{Co}^{57}$  in Ni. A paramagnetic hydride component along with the original ferromagnetic  $\text{Co}^{57}$ -nickel spectrum was observed after cathodic treatment of the specimens. The amount of hydride phase increased with increasing electrolysis time. The chemical shift of the hydride indicated an increase in the 3d-population by 0.35 electrons. Similar studies with other metals and alloys should be possible with emission spectroscopy.

#### CONCLUSIONS

The experimental methods and results that were presented above indicate that Mössbauer spectroscopy provides a unique means for studying corrosion behavior. Depending upon the specific technique employed, it is possible to study corrosion from the formation of the first atomic layer to the development of corrosion layers several thousand Angstroms thick. In some cases experiments can be designed for investigations *in situ*. Although studies at present are essentially limited to iron, tin, cobalt and alloys containing these elements, both applied research and fundamental studies are possible for a wide range of practical materials.

The capability of Mössbauer spectroscopy for studying corrosion has been adequately demonstrated, however, application of the technique has not been extensive. It is interesting, therefore, to consider the prospects for further applications in addition to the studies reviewed here. The ability to measure the relative amounts of  $\text{Fe}_3\text{O}_4$  and  $\text{Fe}_2\text{O}_3$  in the oxide coating allows determination of the boundary position as a function of oxidation conditions and thermal treatments. This information along with other data may permit better estimates of ionic mobilities. Since *in situ* studies can be performed, it is possible to learn more about the mechanisms of passivity and the action of corrosion inhibitors. The presence of intermetallic compounds at surfaces, such as  $\text{FeSn}_2$ , has been suggested to induce corrosion inhibition<sup>29</sup>. Mössbauer spectroscopy can be used to detect such intermetallics and to determine the mechanisms of inhibition. In addition, chemical changes at the interface between substrate and coating, such as paint or lacquer, may be followed non-destructively as a function of time.

It appears that the application of Mössbauer spectroscopy to corrosion studies has just started, and we can look forward with anticipation to interesting experiments in the future.

*Acknowledgment.* Support of this research by Army Research Office-Durham is gratefully acknowledged.

#### REFERENCES

1. V. I. Goldanskii and R. H. Herber, *Chemical Applications of Mössbauer Spectroscopy*, Academic Press, New York, 1968.
2. N. N. Greenwood and T. C. Gibb, *Mössbauer Spectroscopy*, Chapman and Hall Ltd., London, 1971.
3. E. J. W. Verwey and P. W. Haayman, *Physica* **8** (1941) 979.
4. J. M. Daniels and A. Rosencwaig, *J. Phys. Chem. Solids* **30** (1969) 1561.
5. D. A. Channing and M. J. Graham, *Corros. Sci.* **12** (1972) 271.
6. A. M. Pritchard and C. M. Dobson, *Nature* **224** (1969) 1295.
7. I. Dezsi, A. Vertes, and L. Kiss, *J. Radioanal. Chem.* **2** (1964) 183.
8. G. M. Bancroft, J. E. O. Mayne, and P. Ridgway, *Brit Corr. J.* **6** (1971) 119.
9. U. Gonser, R. W. Grant, A. H. Muir, Jr., and H. Wiedersich, *Acta Met.* **14** (1966) 259.

10. A. M. Pritchard, J. R. Haddon, and G. N. Walton, *Corros. Sci.* **11** (1971) 11.
11. W. Meisel, *Werkst. Korros.* **21** (1970) 249.
12. R. L. Collins in *Mössbauer Effect Methodology*, Vol. 4, I. J. Gruverman (Editor), Plenum Press, New York, 1968, pp. 129—138.
13. K. R. Swanson and J. J. Spijkerman, *J. Appl. Phys.* **41** (1970) 3155.
14. N. Hershkowitz and J. C. Walker, *Nucl. Instrum. Methods* **53** (1967) 273.
15. J. H. Terrell and J. J. Spijkerman, *Appl. Phys. Lett.* **13** (1968) 11.
16. R. A. Krakowski and R. B. Miller, *Nucl. Instrum. Methods* **100** (1972) 93.
17. V. E. Cosslett and R. N. Thomas, *Brit. J. Appl. Phys.* **15** (1964) 883.
18. G. W. Simmons, E. Kellerman, and H. Leidheiser, Jr., *Corrosion*, in press.
19. H. Onodera, H. Yamamoto, H. Watanabe, and H. Ebiko, *Japan. J. Appl. Phys.* **11** (1972) 1380.
20. Zw. Bonchev, A. Jordanov, and A. Minkova, *Nucl. Instrum. Methods* **70** (1969) 36.
21. H. Pollak, *Phys. Status Solidi* **2** (1962) 270.
22. H. H. Wickman and G. K. Wertheim, in reference [1], pp. 604—614.
23. See reference [2], pp. 329—351.
24. G. K. Wertheim, *Accounts Chem. Research* **4** (1971) 373.
25. M. N. Varma and R. W. Hoffman, *J. Appl. Phys.* **42** (1971) 1727.
26. J. W. Burton and R. P. Godwin, *Phys. Rev.* **158** (1967) 218.
27. F. G. Allen, *Bull. Am. Phys. Soc.* **9** (1964) 926.
28. G. K. Wertheim and D. N. E. Buchanan, *Phys. Lett.* **21** (1966) 255.
29. W. R. Buck, A. N. J. Heyn, and H. Leidheiser, Jr., *J. Electrochem. Soc.* **111** (1964) 386.

## IZVOD

### Primjena Mössbauerove spektroskopije u proučavanju korozije

*H. Leidheiser Jr., G. W. Simmons i E. Kellerman*

Opisani su eksperimentalne metode i rezultati, koji su dobiveni primjenom Mössbauerove spektroskopije u proučavanju korozije. Metodama transmisije, refleksije i emisije, ili kombinacijom istih, moguće je proučavati procese korozije od formiranja prvog atomskog sloja do dalekih stupnjeva kada su slojevi debeli nekoliko stotina nm. Pokazano je, da je moguće odrediti i relativne koncentracije pojedinih oksidnih faza u korozionom sloju. Moguća je i primjena *in situ*, a isto je tako moguća i nedestruktivna primjena na površinu između metala i neke zaštitne prevlake.

CENTER FOR SURFACE  
AND  
COATINGS RESERCH  
LEHIGH UNIVERSITY  
BETHLEHEM, PA., U.S.A.

Primljeno 15. siječnja 1973.